HENRY
Hydraulic Engineering Repository

Ein Service der Bundesanstalt für Wasserbau

Conference Paper, Published Version

Duan, Jennifer G.; Yu, Chunshui

On Numerical Methods for Solving Kinematic Wave Equation

Zur Verfügung gestellt in Kooperation mit/Provided in Cooperation with:
Kuratorium für Forschung im Küsteningenieurwesen (KFKI)

Verfügbar unter/Available at: https://hdl.handle.net/20.500.11970/109742

Vorgeschlagene Zitierweise/Suggested citation:
Duan, Jennifer G.; Yu, Chunshui (2012): On Numerical Methods for Solving Kinematic Wave Equation. In: Hagen, S.; Chopra, M.; Madani, K.; Medeiros, S.; Wang, D. (Hg.): ICHE 2012. Proceedings of the 10th International Conference on Hydroscience & Engineering, November 4-8, 2012, Orlando, USA.

Standardnutzungsbedingungen/Terms of Use:

Die Dokumente in HENRY stehen unter der Creative Commons Lizenz CC BY 4.0, sofern keine abweichenden Nutzungsbedingungen getroffen wurden. Damit ist sowohl die kommerzielle Nutzung als auch das Teilen, die Weiterbearbeitung und Speicherung erlaubt. Das Verwenden und das Bearbeiten stehen unter der Bedingung der Namensnennung. Im Einzelfall kann eine restriktivere Lizenz gelten; dann gelten abweichend von den obigen Nutzungsbedingungen die in der dort genannten Lizenz gewährten Nutzungsrechte.

Documents in HENRY are made available under the Creative Commons License CC BY 4.0, if no other license is applicable. Under CC BY 4.0 commercial use and sharing, remixing, transforming, and building upon the material of the work is permitted. In some cases a different, more restrictive license may apply; if applicable the terms of the restrictive license will be binding.

ON NUMERICAL METHODS FOR SOLVING KINEMATIC WAVE EQUATION

Jennifer G. Duan[1] and Chunshui Yu[2]

ABSTRACT

This paper compares the fifth-order WENO finite volume scheme, the second-order MacCormack finite difference scheme, and the second-order MUSCL finite volume scheme for solving one-dimensional kinematic wave equation. The stability, accuracy, and computational cost of these schemes are compared. These numerical schemes are tested against several synthetic flow experiments including shock wave, rarefaction wave, wave steepening, and uniform/non-uniform rainfall-runoff generated overland flows. The results show that the Godunov-type schemes are more accurate and stable than the classical MacCormack scheme. Furthermore, the Godunov-type schemes, like MUSCL and WENO scheme, are suitable for solving complex flow features using moderated computing resources on current personal computers.

1. INTRODUCTION

The kinematic wave equation was developed by Lighthill and Whitham (1955). The equation is based on the assumptions that the acceleration term and the pressure gradient term in the momentum equation are negligible, so that the energy slope is equal to the bottom slope. The kinematic wave model is widely used to simulate the overland flow (Ponce 1991, Singh 2001). Lighthill and Whitham (1955) found that the kinematic wave dominates the flood wave and can carry the main disturbance to the downstream. Henderson (1966) showed that natural flood waves behave nearly the same as kinematic waves in steep slope ($S_0 > 0.002$). Woolhiser and Liggett (1967) derived the kinematic wave number (k) as a criterion to evaluate the accuracy of the kinematic wave solution and proved that the kinematic wave equation gives accurate results for most overland surface flows. Vieira (1983) concluded that the kinematic wave equation can be used on natural slopes with $k >> 50$. Ponce (1991) compared the kinematic wave equation with the unit hydrograph as a practical method of overland flow routing. Singh (2001) summarized the applicability of kinematic wave equation in hydrology and related areas.

The kinematic wave equation is a first-order hyperbolic partial differential equation (PDE). For a hyperbolic equation, the disturbance will travel along the characteristics of the equation in a finite propagation speed. This feature distinguishes the hyperbolic equations from elliptic and parabolic equations. On the other hand, the kinematic wave equation also belongs to a kind of equations called conservation laws (LeVeque 2002, Toro 2009). Since the flux term is a nonlinear function of conservative variables, the solution does not propagate uniformly but deforms as it evolves. Even the initial conditions are continuous and smooth the hyperbolic conservation laws can develop discontinuities in the solution, for example shock waves.

Both shock wave and rarefaction wave are the intrinsic features of hyperbolic equations. Lighthill and Whitham (1955) discussed the formations of shock wave and rarefaction wave. Kibler and Woolhiser (1970) investigated the structure and general properties of shock waves and developed a numerical procedure for shock fitting. Eagleson (1970) found that using non-uniform flow depth as initial condition, non-uniform rainfall in the source term, or increasing inflows as the boundary condition may cause the formation of kinematic shock wave. Borah and Prasad (1980) presented the propagating shock-fitting scheme (PSF)to simulate overland flow with shock waves. Ponce (1991) summarized four physical conditions necessary for the occurrence of kinematic shock waves. Singh (2001) reviewed the formation and determination of kinematic shock waves.

Due to the complex geometry, non-uniform roughness and non-uniform rainfall pattern, it is impossible to derive a general analytical solution for the kinematic wave equation. Ponce (1991) reviewed the presence of numerical diffusion and numerical dispersion using the finite difference schemes. Singh (2001) summarized three numerical techniques for solving the kinematic wave equation: (1) method of characteristic, (2) finite difference method, and (3) finite element method. Kazezyılmaz-Alhan *et al.* (2005) compared the performance of several finite difference schemes and recommended the MacCormack scheme as a preferred solution technique over other finite difference schemes.

Recently, the Godunov-type finite volume method has been widely used in solving shallow water equations (LeVeque 2002, Toro 2009) because of its wide applicability, strong stability, and high accuracy. One of the most popular Godunov-type methods is a second-order, TVD (Total Variation Diminishing) scheme, namely the MUSCL (Monotone Upstream-centered Schemes for Conservation Laws) scheme (van Leer 1979). The MUSCL scheme is a high-resolution scheme because (1) the spatial accuracy of the scheme is equal to or higher than second order; (2) the scheme is free from numerical oscillations or wiggles; (3) high-resolution is produced around discontinuities. In general, the high-resolution schemes are considered as a tradeoff between computational cost and desired accuracy (Toro 2009, Harten 1983).

Another popular but relatively new method is the high-order WENO (Weighted Essentially Non-Oscillatory) finite volume scheme (Shu 1999). High-order means the order of accuracy is equal to or higher than third-order accuracy. According to Shu (2009), the WENO scheme is suitable for the complicated problems, such as flow having both shocks and complicated smooth structures (e.g., small perturbation). Although the computational cost of high-order WENO scheme can be 3 to 10 times than a second-order high-resolution scheme, it is still preferable because of its high-order accuracy in both time and space.

This study compares the Godunov-type finite volume method using MUSCL scheme and WENO scheme with the finite difference method using MacCormack scheme. The paper is organized as follows: Section 2 introduces the kinematic wave equation and its analytical solutions; Section 3 discusses the numerical schemes: the MacCormack scheme, the MUSCL scheme and the WENO scheme; Section 4 shows the results of typical test cases. Finally, several concluding remarks are given in section 5.

2. GOVERNING EQUATIONS

The one dimensional kinematic wave equation for flows over a slope is given by (Lighthill, et al., 1955, Eagleson, 1970):

$$\frac{\partial h}{\partial t}+\frac{\partial q}{\partial x}=i_0 \tag{1}$$

where h is the depth of flow; q is the discharge per unit width; $i_0 = i - f$ is the rain excess; i is the intensity of rainfall; f is the infiltration rate; t is the time; x is the downslope distance.

For the overland flow, the discharge q is defined as:

$$q = \alpha h^m \tag{2}$$

where m is the exponential, and α is the coefficient. For fully turbulent flow, the coefficients are given by Ponce (1989):

$$\alpha = \frac{1}{n}\sqrt{S_0},\ m = \frac{5}{3} \tag{3}$$

where n is the Manning's roughness coefficient; S_0 is the bottom slope. It is obvious that the flux function $q(h)$ is a convex function (Toro 2009, Jacovkis *et al.* 1996) because the second order derivative is positive:

$$\frac{d^2q}{dh^2} = \alpha m(m-1)h^{m-2} > 0, \text{ for } h > 0 \tag{4}$$

The one dimensional kinematic wave equation can be solved by the method of characteristics (Eagleson 1970, Kazezyılmaz-Alhan *et al.* 2005).The analytical solution is to calculate the outflow hydrograph at the downstream end of the domain ($q = q_L, x = L$) in response to the rainfall excess within a specified duration.

Given a constant rainfall excess (i_0) and the following initial condition

$$h = 0 \ (t = 0 \text{ and } 0 \le x \le L) \tag{5}$$

and the boundary condition,

$$h = 0 \ (t > 0 \text{ and } x = 0) \tag{6}$$

The two possible outflow hydrographs are:

Case 1 ($t_r \ge t_c$):

$$q_L = \alpha h_L^m, \text{ to solve } h_L \text{ use: } \begin{cases} h_L = i_0 t, \text{ for } t \le t_c \\ h_L = i_0 t_c, \text{ for } t_c < t \le t_r \\ L = \alpha h_L^{m-1}[h_L i_0^{-1} + m(t - t_r)], \text{ for } t > t_r \end{cases} \tag{7}$$

Case 2 ($t_r < t_c$):

$$q_L = \alpha h_L^m, \text{ to solve } h_L \text{ use: } \begin{cases} h_L = i_0 t, \text{ for } t \le t_r \\ h_L = i_0 t_r, \text{ for } t_r < t \le t_p \\ L = \alpha h_L^{m-1}[h_L i_0^{-1} + m(t - t_r)], \text{ for } t > t_p \end{cases} \quad (8)$$

where t_r is the duration of rainfall, and t_c is the time of concentration:

$$t_c = \left(\frac{L i_0^{1-m}}{\alpha} \right)^{1/m} \quad (9)$$

and t_p is defined as:

$$t_p = t_r + \frac{t_c^* - t_r}{m}, \; t_c^* = \frac{L}{\alpha h_{Lr}^{m-1}}, \; h_{Lr} = i_0 t_r \quad (10)$$

3. NUMERICAL SCHEMES

Since the kinematic wave equation is a nonlinear hyperbolic partial differential equation, different numerical schemes exhibit different amounts of numerical diffusion and dispersion depending on the nature of schemes. Numerical diffusion often presents itself as the attenuation of the kinematic wave, while numerical dispersion is responsible for oscillations or negative outflows near large gradients. Ponce (1991) discussed intrinsic numerical diffusion and dispersion of finite difference schemes. Kazezyılmaz-Alhan *et al.* (2005) evaluated several finite difference schemes for solving kinematic wave equation: the linear explicit scheme, the four-point Pressimann implicit scheme, and the MacCormack scheme. The study (Kazezyılmaz-Alhan *et al.* 2005) recommended the second-order MacCormack scheme is preferable to the second-order four-point implicit scheme. However, Kazezyılmaz-Alhan *et al.* (2005) did not test the currently popular Godunov-type finite volume schemes (LeVeque 2002, Toro 2009), which is suitable for solving the nonlinear hyperbolic equations. To provide comparisons with classical finite difference schemes, a study of two high-resolution Godunov-type finite volume schemes, the MUSCL finite volume scheme and the WENO finite volume scheme, is presented in this paper. All the selected schemes are explicit, but differ in order of accuracy. The MUSCL scheme is a second-order scheme while the WENO scheme is fifth-order.

3.1 MacCormack Finite Difference Scheme

The MacCormack scheme (MacCormack 2003) is a commonly used Lax-Wendroff type finite difference scheme to solve hyperbolic PDEs. This two-step scheme is second-order accurate in both time and space. Compared to the first-order scheme, the MacCormack scheme does not introduce

numerical diffusions in the solution. However, the numerical dispersions can be introduced in the region of large gradients.

The MacCormack scheme is a variation of the two-step Lax-Wendroff scheme. It includes two steps: a predictor step followed by a corrector step. The predictor step uses forward difference approximations while the corrector step uses backward difference approximations for spatial derivatives. The order of differencing can be reversed from time step to time step (i.e., forward/backward differencing followed by backward/forward differencing). The time step used in the predictor step is Δt in contrast to $\Delta t/2$ used in the corrector step.

Predictor step:

$$h_i^{\overline{n+1}} = h_i^n - \frac{\Delta t}{\Delta x}(q_{i+1}^n - q_i^n) + i_0 \Delta t \tag{11}$$

Corrector step:

$$h_i^{n+1} = \frac{1}{2}(h_i^n + h_i^{\overline{n+1}}) - \frac{1}{2}\left[\frac{\Delta t}{\Delta x}(q_i^{\overline{n+1}} - q_{i-1}^{\overline{n+1}}) + i_0 \Delta t\right] \tag{12}$$

where subscript i is the spatial index; superscript n, $\overline{n+1}$, and $n+1$ are the temporal indices; Δt is time step; Δx is the space step.

3.2 MUSCL Finite Volume Scheme

The MUSCL scheme was introduced by van Leer (1979). It's the first second-order TVD Godunov-type finite volume scheme. MUSCL uses piecewise linear approximation to reconstruct the depths at the interfaces of cells:

$$h_{i+1/2} = h_i + \nabla h_i \cdot r_{i+1/2} \tag{13}$$

where h_i is flow depth at the center of cell i; $h_{i+1/2}$ is the reconstructed depth at the interface $i+1/2$ of cell; ∇h_i is the limited depth gradient of cell i; $r_{i+1/2}$ is the distance from the cell center to the interface $i+1/2$.

The limited gradients can be calculated by several slope limiters (Minmod, Superbee, etc.). Here the van Leer limiter(van Leer 1974, Causon *et al.* 2000) is used in the study:

$$\nabla h = \frac{\nabla h_L |\nabla h_R| + |\nabla h_L| \nabla h_R}{|\nabla h_L| + |\nabla h_R|} \tag{14}$$

where $\nabla h_L = \frac{h_i - h_{i-1}}{\Delta x}$ and $\nabla h_R = \frac{h_{i+1} - h_i}{\Delta x}$.

The local Lax-Friedrichs (LLF) method (LeVeque,2002) is used to calculate the fluxes across the cell interfaces:

$$Q_{i-1/2} = \frac{1}{2}\left[q_{i-1} + q_i - a_{i-1/2}(h_i - h_{i-1})\right] \tag{15}$$

$$a_{i-1/2} = \max(|c_{i-1}|, |c_i|) \tag{16}$$

where c is the celerity and defined in (25).

Based on calculated numerical fluxes across the interfaces, the solution can be updated by a time marching method. Instead of using the predictor-corrector method of MUSCL-Hancock scheme, the second-order TVD Runge-Kutta method (Gottlieb *et al.* 1998) is employed in the study to discretize the time derivative.The second-order TVD Runge-Kutta method (RK2) can be written as:

$$\begin{aligned} h^{(1)} &= h^n + \Delta t \cdot L_i(h^n) \\ h^{n+1} &= \frac{1}{2}h^n + \frac{1}{2}h^{(1)} + \frac{1}{2}\Delta t \cdot L(h^{(1)}) \end{aligned} \tag{17}$$

where the operator $L(h)$ is defined as:

$$L(h) = -\frac{1}{\Delta x}\sum Q(h) + i_0 \tag{18}$$

For a TVD Runge-Kutta method, it is guaranteed that each intermediate solution also satisfies the TVD criteria to avoid spurious oscillations in the solution. Because of this, it is a better choice to incorporate a TVD Runge-Kutta method for solving hyperbolic problems.

3.3 WENO Finite Volume Scheme

The first WENO scheme was provided by Liu *et al.*(1994). Jiang *et al.*(1996) presented a general framework to construct arbitrary high order WENO schemes. Details about WENO schemes can be found in Shu(1999, 2009). Instead of using the piecewise linear reconstruction procedure in the MUSCL scheme, the WENO finite volume scheme uses the WENO reconstruction procedure to obtain an approximated function value at the cell interface. The WENO reconstruction procedure consists of four steps:

Step 1. Calculate the smoothness indicators:

$$\begin{cases} \beta_1 = \dfrac{13}{12}(h_{i-2} - 2h_{i-1} + h_i)^2 + \dfrac{1}{4}(h_{i-2} - 4h_{i-1} + 3h_i)^2 \\ \beta_2 = \dfrac{13}{12}(h_{i-1} - 2h_i + h_{i+1})^2 + \dfrac{1}{4}(h_{i-1} - h_{i+1})^2 \\ \beta_3 = \dfrac{13}{12}(h_i - 2h_{i+1} + h_{i+2})^2 + \dfrac{1}{4}(3h_i - 4h_{i+1} + h_{i+2})^2 \end{cases} \tag{19}$$

Step 2. Calculate the third-order approximations at cell interfaces:

$$\begin{cases} h_{i+1/2}^{(1)} = \dfrac{1}{3}h_{i-2} - \dfrac{7}{6}h_{i-1} + \dfrac{11}{6}h_i \\ h_{i+1/2}^{(2)} = -\dfrac{1}{6}h_{i-1} + \dfrac{5}{6}h_i + \dfrac{1}{3}h_{i+1} \\ h_{i+1/2}^{(3)} = \dfrac{1}{3}h_i + \dfrac{5}{6}h_{i+1} - \dfrac{1}{6}h_{i+2} \end{cases} \tag{20}$$

Step 3. Calculate the nonlinear weights:

$$w_j = \frac{\widetilde{w}_j}{\widetilde{w}_1 + \widetilde{w}_2 + \widetilde{w}_3}, \text{ with } \widetilde{w}_j = \frac{\gamma_j}{(\varepsilon + \beta_j)^2}, j = 1,2,3 \tag{21}$$

where $\varepsilon = 10^{-6}$ for actual calculations; γ_j is the linear weights, and is given by:

$$\gamma_1 = \frac{1}{16},\ \gamma_2 = \frac{5}{8},\ \gamma_3 = \frac{5}{16} \tag{22}$$

Step 4. Calculate the fifth-order approximation as a convex combination of the three third-order approximations:

$$h_{i+1/2} = w_1 h_{i+1/2}^{(1)} + w_1 h_{i+1/2}^{(2)} + w_1 h_{i+1/2}^{(3)} \tag{23}$$

The derivative in time is discretized by the third-order TVD Runge-Kutta method(Gottlieb *et al.* 1998), which is a three-step method:

$$\begin{aligned} h^{(1)} &= h^n + \Delta t \cdot L(h^n) \\ h^{(2)} &= \frac{3}{4}h^n + \frac{1}{4}h^{(1)} + \frac{1}{4}\Delta t \cdot L(h^{(1)}) \\ h^{n+1} &= \frac{1}{3}h^n + \frac{2}{3}h^{(2)} + \frac{2}{3}\Delta t \cdot L(h^{(2)}) \end{aligned} \tag{24}$$

where the operator $L(h)$ is given by equation (18).

4. RESULTS

This section evaluates the selected schemes in a variety of flow conditions because a given scheme does well for a test case does not guarantee it will do well for another test case. In order to evaluate the performances of these schemes, it is necessary to choose test cases with exact solutions. For this reason, the one-dimensional propagations of a shock wave and a rarefaction wave are selected. Then the behaviors of these schemes in a long time period are tested by a wave steepening example. Finally, two synthetic rainfall-runoff cases are selected to demonstrate the actual performance of different schemes.

4.1 Shock Wave

The shock wave and rarefaction wave are the intrinsic features of the hyperbolic equations, so does the kinematic wave equation. The celerity of kinematic wave is defined as (Lighthill *et al*. 1955):

$$c = \alpha m h^{m-1} = mv \tag{25}$$

where v is flow velocity. Consider the following initial-value problem for the kinematic wave equation:

$$h(x,0) = \begin{cases} h_L, \text{ if } x < x_0 \\ h_R, \text{ if } x > x_0 \end{cases} \tag{26}$$

If we assume $h_L > h_R$, we will have $c_L > c_R$.This means that a shock wave will arise. The exact shock wave solution for the kinematic wave equation is:

$$h(x,t) = \begin{cases} h_L, \text{ for } (x - x_0)/t < S \\ h_R, \text{ for } (x - x_0)/t > S \end{cases} \tag{27}$$

where S is the shock wave speed. For the kinematic wave equation, according to the Rankine-Hugoniot jump condition (Toro, 2009), S is equal to:

$$S = \alpha \frac{h_R^m - h_L^m}{h_R - h_L} \tag{28}$$

In the study, the following parameters are used: the channel length $L = 10.0$ m; the bed slope $S_0 = 0.0016$; the Manning's coefficient $n = 0.025$ s/m$^{1/3}$; the simulation time $t = 3.5$ s; the time step $\Delta t = 0.01$ s; the grid spacing $\Delta x = 0.1$ m. The initial condition is: $h_L = 1.0$ m and $h_R = 0.5$ m. The boundary conditions are zero-depth gradient at both the entrance and the exit of the channel.

The flow depth profiles calculated by the numerical schemes and the exact solution are plotted in **Error! Reference source not found.**. The results show that the numerical diffusions near

the front of shock wave are small for all the numerical schemes. But the numerical dispersion using the MacCormack finite difference is large. Many wiggles are generated near the wave front.

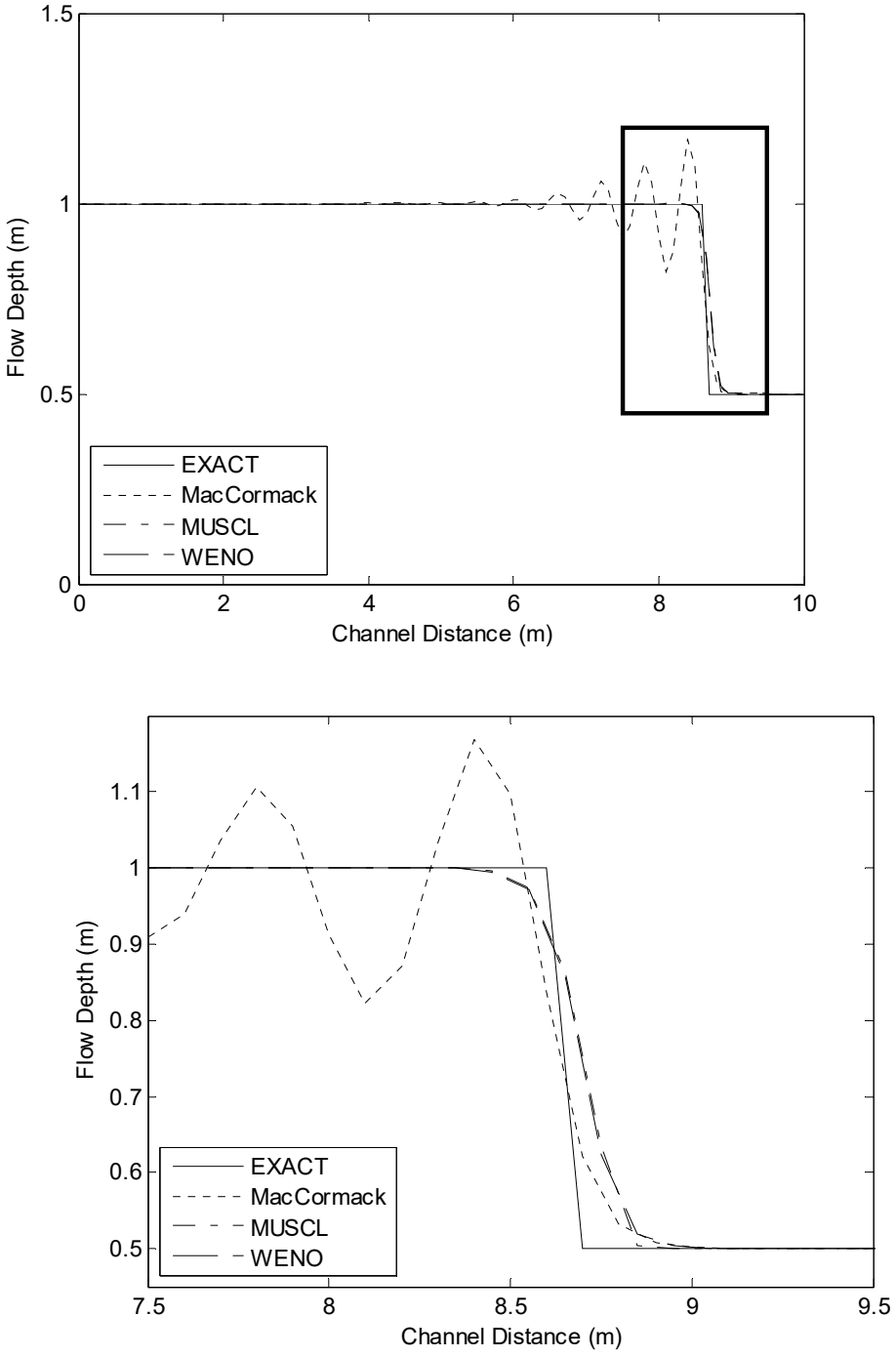

Figure 1 Results of shock wave test case. (Above: global view. Bottom: zoom view.)

4.2 Rarefaction Wave

Reconsider the initial-value problem described in Eq.(26), and assume $h_L < h_R$, we have $c_L < c_R$. This time, instead of generating a shock wave, a rarefaction wave is generated near the discontinuity since the celerity at the head of the discontinuity is greater than that at the tail and, consequently, the

discontinuity continually expands as it propagates. For the kinematic wave equation, the exact solution of rarefaction wave is:

$$h = \begin{cases} h_L, \text{ for } \dfrac{x - x_0}{t} < c_L \\ h_L + (\dfrac{x - x_0}{t} - c_L)\dfrac{h_R - h_L}{c_R - c_L}, \text{ for } c_L \le \dfrac{x - x_0}{t} \le c_R \\ h_R, \text{ for } \dfrac{x - x_0}{t} > c_R \end{cases} \tag{29}$$

The parameters used in the rarefaction test case are summarized as: the channel length $L = 10.0$ m; the bed slope $S_0 = 0.0016$; the Manning's coefficient $n = 0.025$ s/m$^{1/3}$; the simulation time $t = 3.0$ s; the time step $\Delta t = 0.01$ s; and the grid spacing $\Delta x = 0.1$ m. The initial condition is: $h_L = 0.5$ m and $h_R = 1.0$ m. The boundary conditions are zero-depth gradient at both ends of the channel.

The calculated profiles are plotted in **Error! Reference source not found.**. The results are similar to the shock wave case: the MacCormack scheme generated notable oscillations at the tail of the rarefaction wave. Taylor *et al.* (1972) tested the MacCormack scheme for solving the Burgers' equation and found that the MacCormack scheme is unstable for rarefaction wave under some conditions. This study finds that the same phenomenon occurred to kinematic wave equation. The reason is that the oscillations lie in the lower flow depth part of the rarefaction wave instead of higher part of the shock wave. This makes it easy to get unrealistic negative depth values in the case of rarefaction waves. Therefore, for the rarefaction wave, the MacCormack scheme is not as stable as the MUSCL scheme or the WENO scheme.

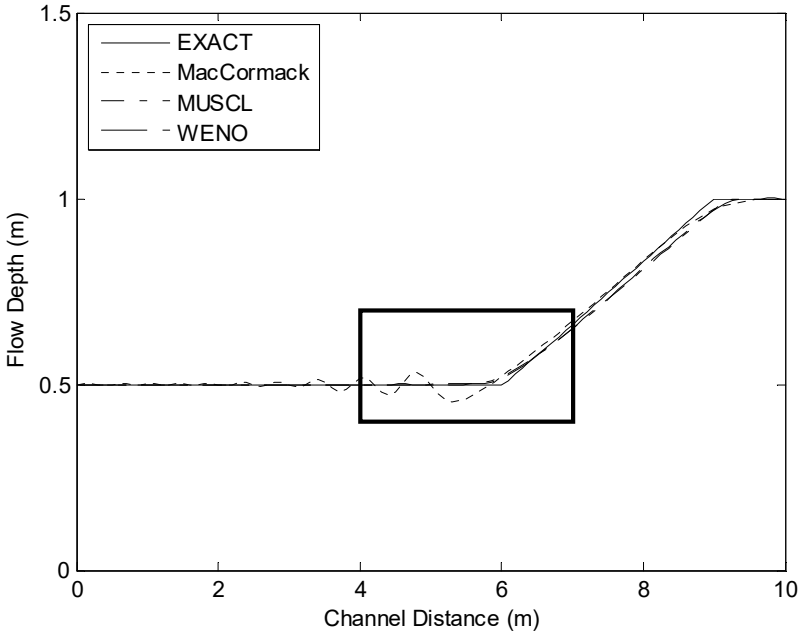

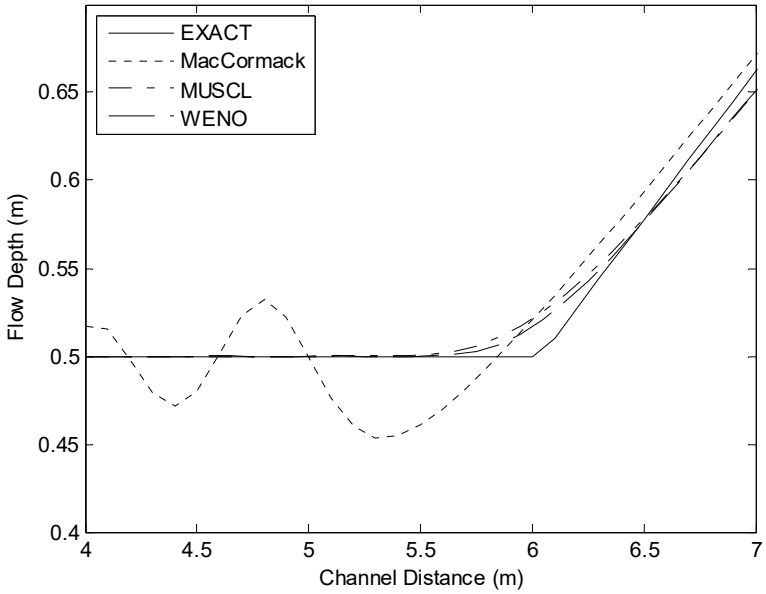

Figure 2 Results of rarefaction wave test case. (Above: global view. Bottom: zoom view.)

4.3 Wave Steepening

One of the prominent features of the hyperbolic equation is that discontinuities will be generated even the initial water surface is smooth. So it's important for a scheme to preserve the sharpness of discontinuous fronts in a long-time simulation. This test case is to test the long time behavior of the schemes, especially the ability of anti-diffusion.

Here are the parameters in the test case: the channel length $L = 10.0$ m; the bed slope $S_0 = 0.0016$; the Manning's coefficient $n = 0.025$ s/m$^{1/3}$; the simulation time $t = 100.0$ s; the time step $\Delta t = 0.01$ s; and the grid spacing $\Delta x = 0.1$ m. The initial condition is:

$$h = \max\left[\ 0.5,\ \ 1.0-(x-1.0)^2\ \right] \tag{30}$$

This initial condition will create a parabolic perturbation in the channel (**Error! Reference source not found.**). The boundary conditions are periodic flow depths at both ends of the channel.

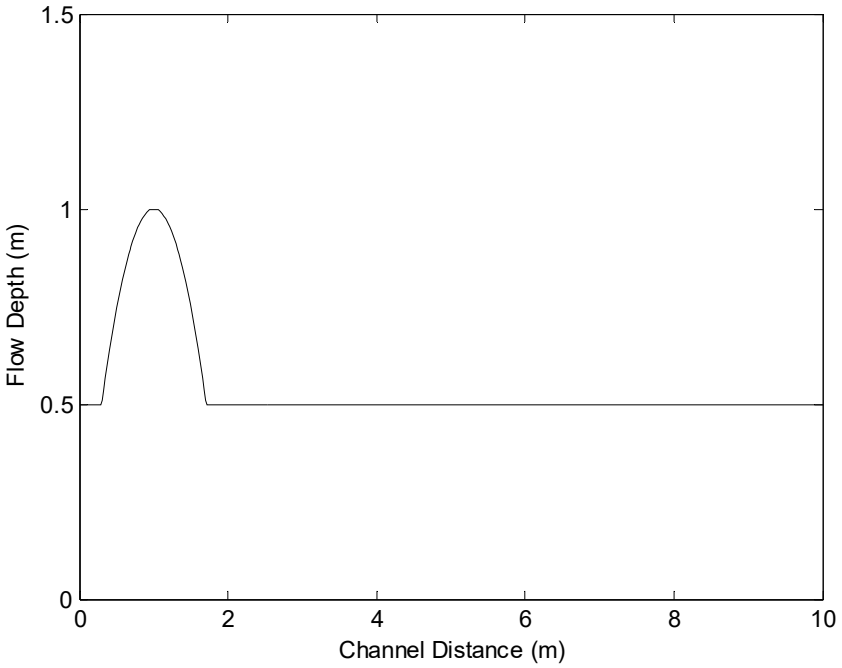

Figure 3 Initial condition of long time evolution case.

The parabolic perturbation will produce a "wave steepening" effect in the domain (Henderson 1966, Toro 2009). The reason is that the celerity of the perturbation is faster than the ambient fluid. The head of the perturbation is a compressive region while the tail of the perturbation is an expansive region. This perturbation is a combination of a shock wave (head) and a rarefaction wave (tail). This scenario is detrimental to the MacCormack scheme because the oscillations occurred behind the shock wave will drown out the parabolic perturbation immediately (**Error! Reference source not found.**).

The results of MUSCL scheme and WENO scheme are plotted in **Error! Reference source not found.**. After 100 seconds, the fronts of the perturbation are still sharp. The numerical diffusion of the MUSCL scheme is a little larger than that of the WENO scheme because the MUSCL scheme is a second-order scheme while the WENO scheme is third-order accurate near the discontinuity.

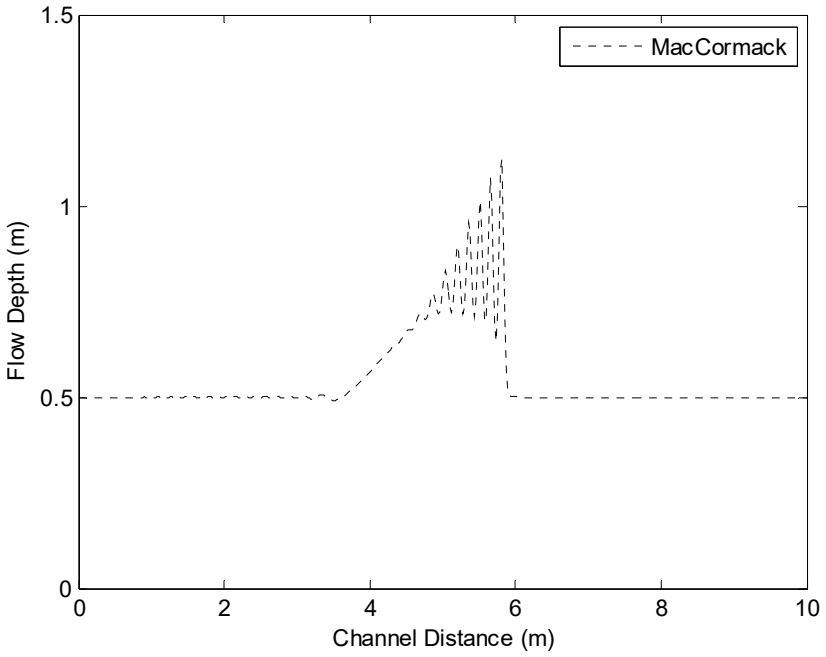

Figure 4 Oscillations of the MacCormack scheme. (number of nodes = 501, t = 2.0 s)

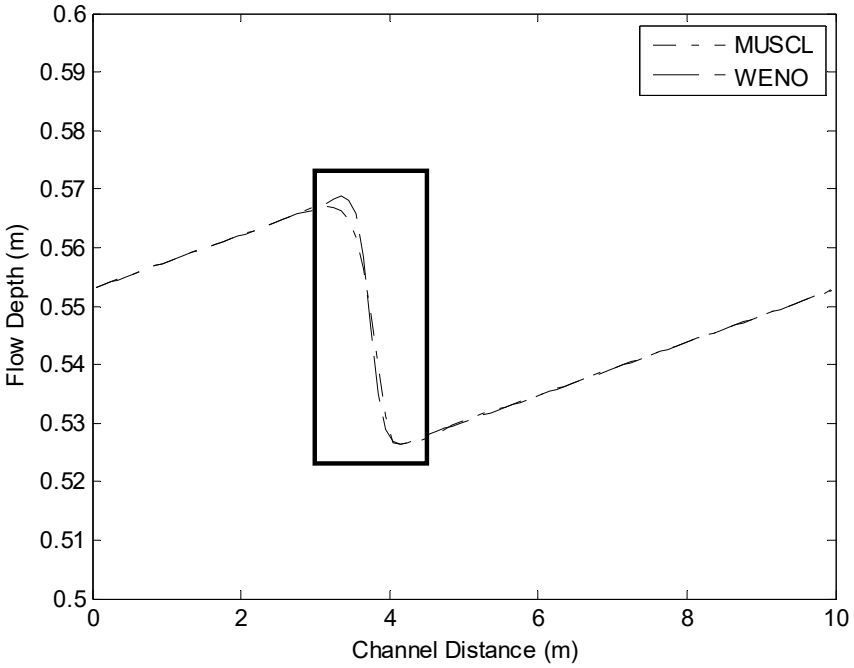

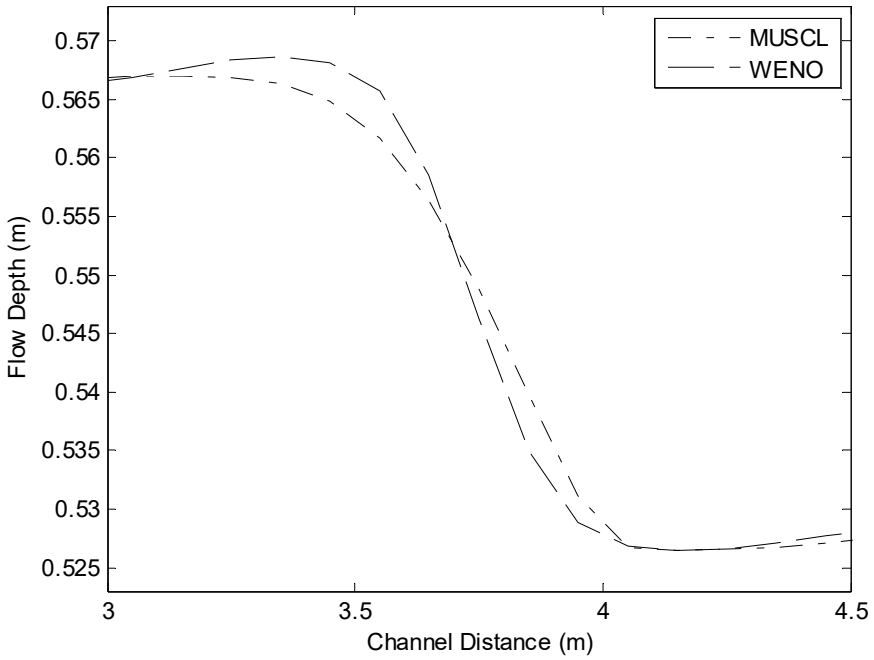

Figure 5 Results of wave steepening test case. (Above: global view. Bottom: zoom view)

4.4 Uniform Rainfall-runoff Overland Flow

The test case is presented by Kazezyılmaz-Alhan *et al.*(2005) to test the rainfall-runoff overland flow. For this case, the duration of rainfall is longer than the time of concentration ($t_r \geq t_c$). The parameters are listed here: the channel length $L = 182.88$ m; the bed slope $S_0 = 0.0016$; the Manning's coefficient $n = 0.025$ s/m$^{1/3}$; the duration of rainfall $t_r = 0.5$ h; the rainfall excess $i_0 = 50.8$ mm/h; simulation time $t = 1$ h; the time step $\Delta t = 1.0$ s; and the grid spacing $\Delta x = 1.83$ m. The initial condition is $h = 0.0$ m. The boundary conditions are zero-depth gradient at the outlet and zero depth at the inlet.

Error! Reference source not found. plots the outflow hydrographs calculated by the numerical schemes and the exact solution calculated by Eq.(7). Since there isn't any discontinuity/perturbation in the domain, the results obtained by the three numerical schemes are very close to the exact solution. The comparisons of the peak of the hydrographs show that the WENO scheme yields the closest results to the exact solution without any oscillation.

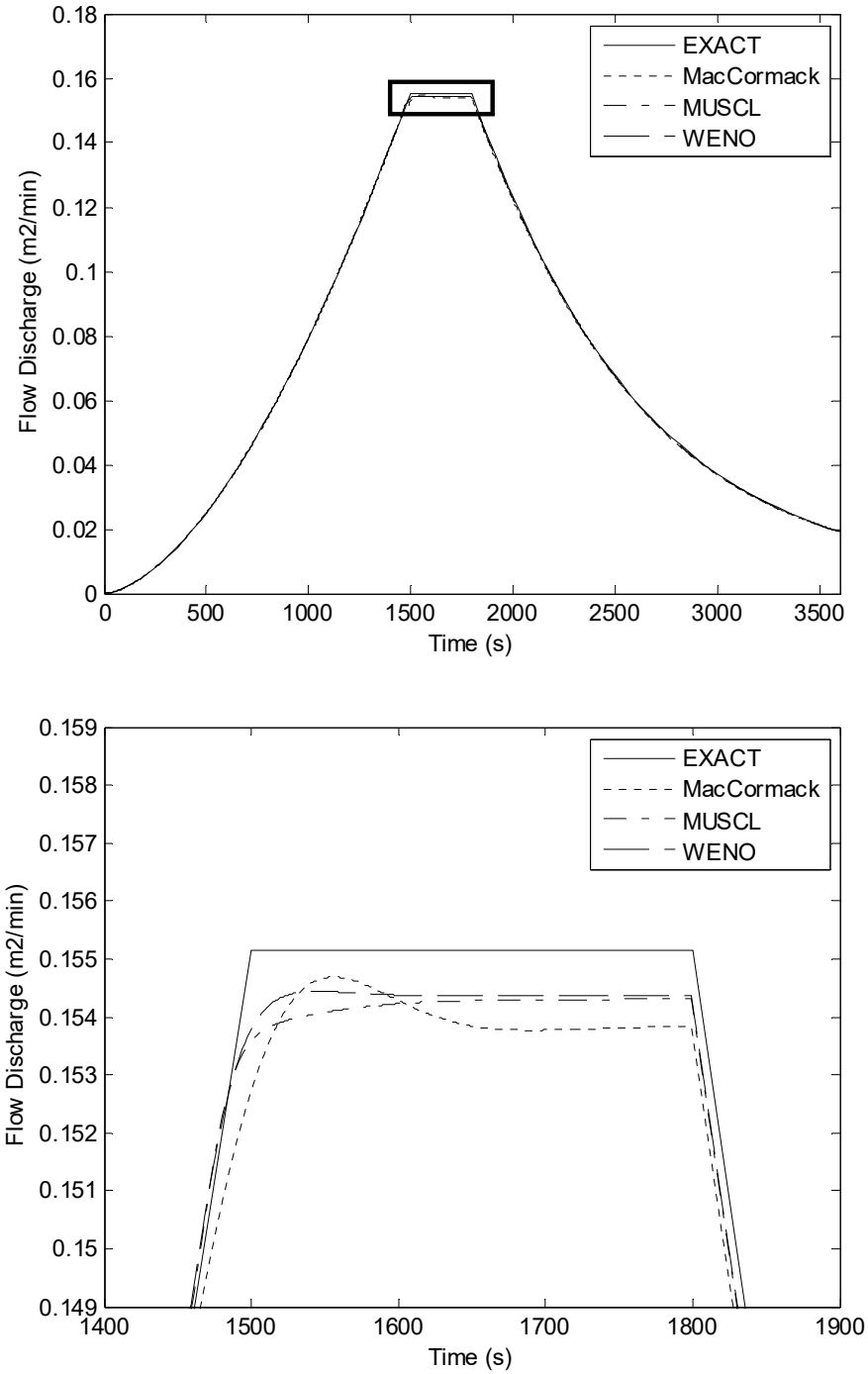

Figure 6 Hydrograph of uniform rainfall-runoff case. (Above: global view. Bottom: zoom view.)

4.5 Steady Non-uniform Rainfall-runoff Overland Flow

To compare the stability of different schemes, a steady non-uniform rainfall-runoff case is tested. The test conditions are the same as the uniform rainfall-runoff case except rainfall excess. The following steady non-uniform rainfall excess is used in this case (**Error! Reference source not found.**):

$$i_0(mm/h) = \begin{cases} 2.0 \times 50.8 - 0.0328 \times 50.8 \times (x - 91.44)^2, \ 73.15m < x < 109.72m \\ 50.8, \ elsewhere \end{cases} \quad (31)$$

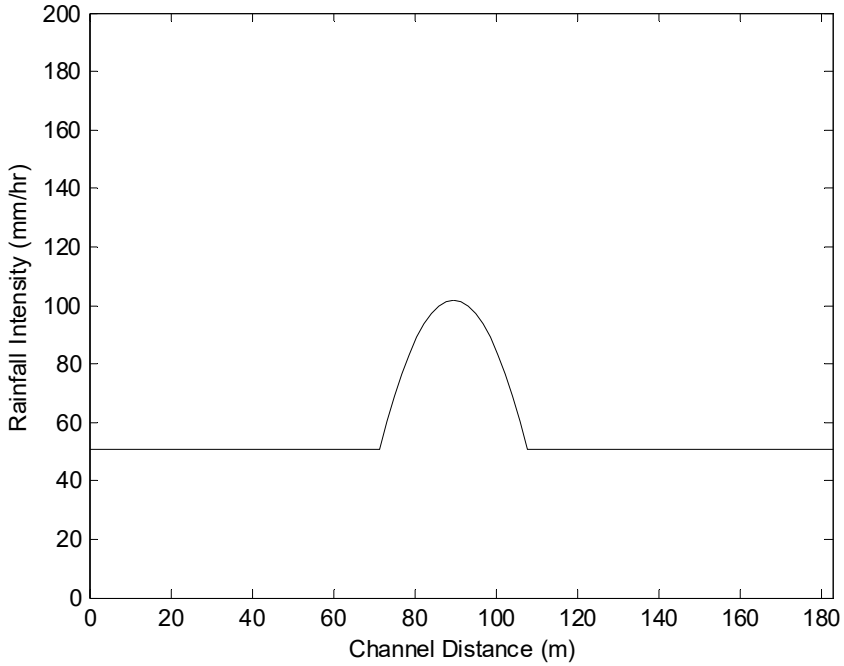

Figure 7 Non-uniform rainfall distribution

The duration of rainfall is infinite. The results are showed in **Error! Reference source not found.** and **Error! Reference source not found.**. The depth of the runoff generated by the non-uniform rainfall is not smoothly distributed and a shock wave is generated. Oscillations occurred in the solution of the MacCormack scheme.

The CPU times of the MacCormack, MUSCL, and WENO schemes are 5.8, 13.5, and 38.7s, respectively. The MacCormack scheme is the fastest scheme. As to the Godunov-type schemes, the WENO scheme is three times slower than the MUSCL scheme. The hardware platform is a DELL XPS notebook (Intel i5 M450 2.4GHz CPU with 4GB memory). The programs are developed using Matlab 2011b running on Microsoft Windows 7.0 OS.

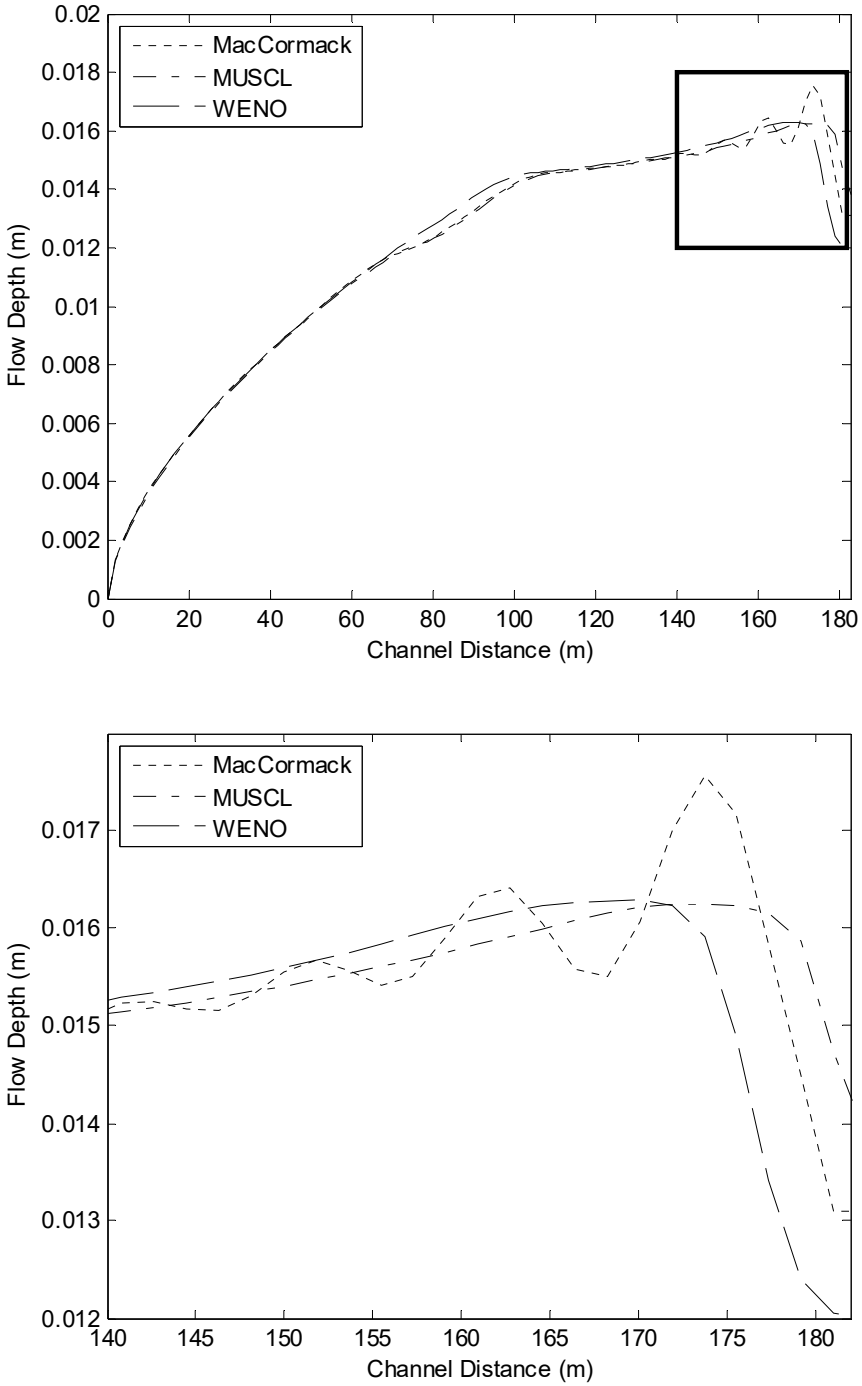

Figure 8 Results of non-uniform rainfall-runoff test case (T=850s). (Above: global view. Bottom: zoom view)

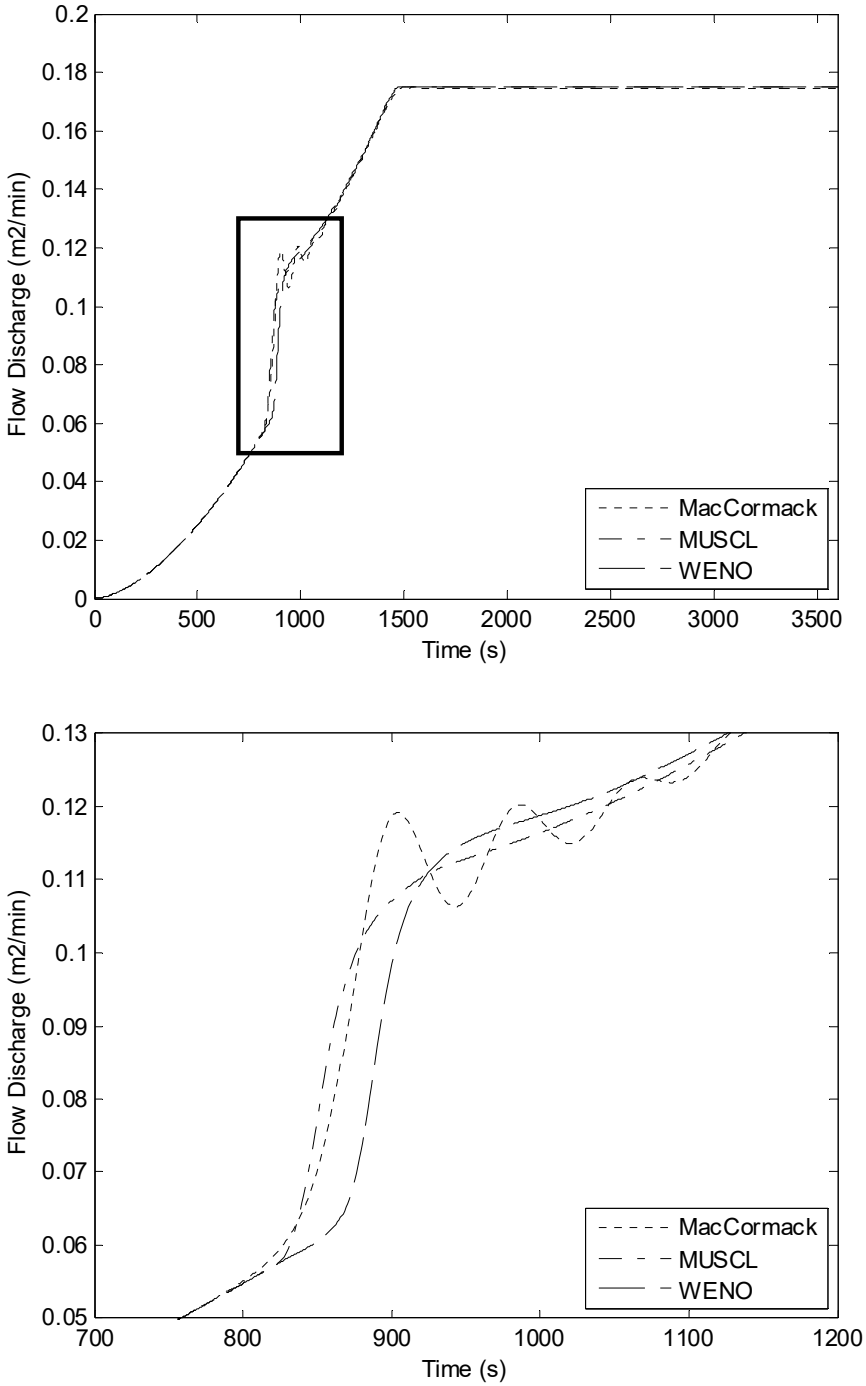

Figure 9 Hydrograph of non-uniform rainfall-runoff test case. (Above: global view. Bottom: zoom view)

5. CONCLUSIONS

In this study, three numerical schemes (MacCormack scheme, MUSCL scheme and WENO scheme) are compared. The schemes are examined by using four test cases which are shock wave, rarefaction wave, wave steepening, and rainfall-runoff overland flow test. The results show that moderate oscillations appear in the solutions using the MacCormack scheme. The oscillations seriously affect the stability of the solution, which makes the scheme could not complete the wave steepening test

case. On the other hand, the Godunov-type finite volume methods present better performance than the finite difference method. There are no oscillations in the solutions using the MUSCL scheme or the WENO scheme. The high-order WENO scheme shows the best resolution power in all test cases. Although the computational costs are higher than the MacCormack scheme's, to ensure numerical stability, we recommend the MUSCL/WENO schemes as the preferred techniques for solving the kinematic wave equation.

ACKNOWLEDGEMENTS

The authors are grateful for research funding provided by NSF Award EAR-0846523 to the University of Arizona. The authors wish to acknowledge in particular Chunyan Gao for valuable discussions on the kinematic wave equation.

REFERENCES

Borah, D. K., Prasad, S. N., and Alonso, C. V. (1980). "Kinematic Wave Routing Incorporating Shock Fitting." *Water Resour Res*, 16(3), 529-541.

Causon, D. M., Ingram, D. M., Mingham, C. G., Yang, G., and Pearson, R. V. (2000). "Calculation of shallow water flows using a Cartesian cut cell approach." *Adv Water Resour*, 23(5), 545-562.

Eagleson, P. S. (1970). *Dynamic hydrology*, McGraw-Hill, New York,.

Gottlieb, S., and Shu, C. W. (1998). "Total variation diminishing Runge-Kutta schemes." *Math Comput*, 67(221), 73-85.

Harten, A. (1983). "High-Resolution Schemes for Hyperbolic Conservation-Laws." *J Comput Phys*, 49(3), 357-393.

Henderson, F. M. (1966). *Open channel flow*, Macmillan, New York,.

Jacovkis, P. M., and Tabak, E. G. (1996). "A kinematic wave model for rivers with flood plains and other irregular geometries." *Math Comput Model*, 24(11), 1-21.

Jiang, G. S., and Shu, C. W. (1996). "Efficient implementation of weighted ENO schemes." *J Comput Phys*, 126(1), 202-228.

Kazezyılmaz-Alhan, C. M., Medina Jr, M. A., and Rao, P. (2005). "On numerical modeling of overland flow." *Applied Mathematics and Computation*, 166(3), 724-740.

Kibler, D. F., and Woolhiser, D. A. (1970). *The kinematic cascade as a hydrologic model*, Colorado State University.

LeVeque, R. J. (2002). *Finite volume methods for hyperbolic problems*, Cambridge University Press, Cambridge ; New York.

Lighthill, M. J., and Whitham, G. B. (1955). "On Kinematic Waves. I. Flood Movement in Long Rivers." *Proceedings of the Royal Society of London. Series A. Mathematical and Physical Sciences*, 229(1178), 281-316.

Liu, X.-D., Osher, S., and Chan, T. (1994). "Weighted Essentially Non-oscillatory Schemes." *J Comput Phys*, 115(1), 200-212.

MacCormack, R. W. (2003). "The effect of viscosity in hypervelocity impact cratering (Reprinted from AlAA Paper 69-354, 1969)." *J Spacecraft Rockets*, 40(5), 757-763.

Ponce, V. M. (1991). "The Kinematic Wave Controversy." *J Hydraul Eng-Asce*, 117(4), 511-525.

Ponce, V. M. (1989). *Engineering hydrology : principles and practices*, Prentice Hall, Englewood Cliffs, N.J.

Singh, V. P. (2001). "Kinematic wave modelling in water resources: a historical perspective." *Hydrol Process*, 15(4), 671-706.

Shu, C. W. (1999). "High order ENO and WENO schemes for computational fluid dynamics." *High-order methods for computational physics*, Deconinck, ed., Springer, 439-582.

Shu, C. W. (2009). "High Order Weighted Essentially Nonoscillatory Schemes for Convection Dominated Problems." *Siam Rev*, 51(1), 82-126.

Toro, E. F. (2009). *Riemann solvers and numerical methods for fluid dynamics : a practical introduction*, Springer, Dordrecht ; New York.

Taylor, T. D., Ndefo, E., and Masson, B. S. (1972). "A study of numerical methods for solving viscous and inviscid flow problems." *J Comput Phys*, 9(1), 99-119.

Woolhise, D. A., and Liggett, J. A. (1967). "Unsteady 1-Dimensional Flow over a Plane - Rising Hydrograph." *Water Resour Res*, 3(3), 753-&.

Taylor, T. D., Ndefo, E., and Masson, B. S. (1972). "A study of numerical methods for solving viscous and inviscid flow problems." *J Comput Phys*, 9(1), 99-119.